JOURNAL
OF THE AMERICAN CHEMICAL SOCIETY

VOLUME 97, NUMBER 8 APRIL 16, 1975

An Extended View of the Benzene 260-nm Transition via Single Vibronic Level Fluorescence. I. General Aspects of Benzene Single Vibronic Level Fluorescence[1,2]

A. E. W. Knight, C. S. Parmenter,* and M. W. Schuyler

Contribution from the Department of Chemistry, Indiana University, Bloomington, Indiana 47401. *Received September 9, 1974*

Abstract: Vapor fluorescence spectra from benzene molecules excited to single vibronic levels or to small groups of levels in the lower 2500 cm^{-1} of the $^1B_{2u}$ state are analyzed. Every fluorescence spectrum supports the Herzberg–Teller description of the $^1B_{2u}$–$^1A_{1g}$ vibronically induced transition. Vibrational quantum changes which follow first- and second-order Herzberg–Teller selection rules, and which involve a consistent set of vibrational modes, account for the bulk of the structure in fluorescence. Fluorescence bands induced by $\Delta v = \pm 1$ quantum changes in the e_{2g} mode ν_6 and which have zero quantum changes in all other nontotally symmetric vibrations exceed the intensity of other transitions by at least a factor of 10. This pattern is observed without exception from every emitting level. Approximate Franck–Condon factor calculations replicate the striking effect which the ν_1 quantum number in the emitting level ($v_1' = 0$, 1, or 2) has on the observed band intensities in ν_1 progressions.

Numerous absorption bands in the $^1B_{2u} \leftarrow {}^1A_{1g}$ ($S_1 \leftarrow S_0$) transition of benzene vapor are sufficiently free of overlap by others so that they can be pumped selectively with tuned narrow band light. By this means S_1 molecules can be prepared with populations strongly biased to a single vibronic level (SVL), and if the gas pressure is low enough, fluorescence will occur before collisions scramble the vibrational energy. This radiative decay is termed SVL fluorescence to distinguish it from the more common low-pressure or "resonance" fluorescence which originates from a molecular ensemble with a distribution of populated vibronic levels.

In principle SVL fluorescence can carry studies of excited state relaxation to a high level of detail. The yields and lifetimes combine to give the absolute rates of both radiative and nonradiative decay as a function of vibrational excitation in the isolated molecule. In turn, modification of those yields and lifetimes as gas pressures increase should allow a state-selected study of collision-induced relaxation. Initial steps toward these possibilities were described in an early report[3] and the promised picture of excited state relaxation in benzene has subsequently begun to emerge. The dependence of both radiative and nonradiative relaxation on vibrational excitation is known[4-10] and probes have even been extended to selective rotational excitation within a vibronic level.[8,11]

Attention is now directed toward another aspect of these benzene experiments, namely the single level fluorescence spectra. They are of particular interest because the symmetry forbidden $^1B_{2u}$–$^1A_{1g}$ radiative transition in benzene has long been considered the classic example of such Herzberg–Teller[12] transitions. The analysis of SVL fluorescence spectra extends considerably the detail with which this vibronically induced radiative transition can be described.

A few SVL spectra from benzene have been discussed in earlier reports. The first[3] plus another[13] outlined their general appearance. The second examined the structure of fluorescence from the zero-point levels of C_6H_6 and C_6D_6.[14] Another used SVL fluorescence as an aid in assigning the low-pressure fluorescence from benzene excited with the 2537 Å Hg line.[15] Finally, an example of the use of SVL fluorescence spectra to elucidate absorption band assignments is included in a review of excited state relaxation in benzene.[16]

A more encompassing description of SVL fluorescence from benzene will now be given with spectra obtained by selective excitation of eight absorption regions. These excitations pump levels comprised of fundamentals, overtones, and combinations of the modes ν_1, ν_6, and ν_{16}. Every level is in the lower 2500 cm^{-1} of the S_1 manifold where the level separation usually exceeds their widths so that the levels are truly discrete. Significant collisional relaxation is precluded by holding the gas pressures near or below 0.15 Torr at room temperature.[17]

The low-light levels encountered in these experiments necessitate a compromise between resolution and data collection time. Most of the fluorescence spectra have been recorded with a resolution of 15–75 cm^{-1} (~0.1 to 0.5 nm). Many of the finer aspects of the band structure are hidden at this resolution, but nevertheless a rich structure is still re-

solved so that the ensemble of spectra provide an improved picture of vibrational activity. A consistent set of selection rules emerge from the analyses. These rules can be applied to predict the fluorescence spectrum expected after excitation to a given vibronic level, or conversely, to identify the emitting level by analyzing the SVL fluorescence spectrum. In the following paper,[18] hereafter referred to as part II, the latter procedure has been used as a probe to test absorption assignments in the $^1B_{2u} \leftarrow {}^1A_{1g}$ transition.

The spectra also yield an extended view of the Franck-Condon factors for the ν_1 progressions which dominate the vibrational structure in both absorption and fluorescence.

Special attention has been given to fluorescence from the zero-point level. The spectrum has been remeasured with an order of magnitude improvement in both resolution and signal-to-noise ratio over the earlier spectrum.[14] Band contours can be identified, and positions of band maxima are located with an accuracy of a few reciprocal centimeters so that even some comparatively weak transitions can be securely assigned.

Experimental Section

Tuned narrow-band exciting light was obtained from a xenon arc coupled with a monochromator. Benzene vapor was held in a vessel containing a set of White-Herzberg mirrors to increase the absorption path length and a set of Welsh mirrors to improve collection of fluorescence. The fluorescence was dispersed with either a 0.75-m scanning spectrometer linear in wavelength and used in second order, or a 1.7-m scanning spectrometer linear in wave number and used in fourth order. Each of these Czerny-Turner spectrometers was equipped with a photomultiplier whose output was monitored with photon counting circuits.

Details of this equipment and the technique are given with references elsewhere.[14,19]

Notation

Band assignments use the notation introduced by Callomon, Dunn, and Mills (CDM).[20] For example, the band $6_0^1 16_1^1 1_0^2$ is a transition in which $v_x = 0$ in both electronic states for all modes except ν_6, ν_{16}, and ν_1. The superscripts indicate that $v_6' = 1$, $v_{16}' = 1$, and $v_1' = 2$ in the upper electronic state and the subscripts indicate in a similar manner the ground state vibrational content. The notation also describes specific levels. For example, $6^1 16^1 1^2$ designates a molecule in the upper electronic state with $v_6' = 1$, $v_{16}' = 1$, and $v_1' = 2$ whereas 16_1 identifies a ground state molecule with $v_{16}'' = 1$.

Absorption bands are also familiarly identified by the system A_1^0, B_0^0, C_0^1, etc., used in Radle and Beck's extensive compilation of band positions[21] and in absorption assignments.[22,23] Following a widespread convention for the $^1B_{2u}$-$^1A_{1g}$ transition, Wilson's labeling of vibrational modes is used. It is related to Herzberg's numbering in Table I where observed vibrational frequencies are listed.

Fluorescence Spectra

The fluorescence spectra shown are linear either in wavelength or wave number with energy increasing to the right. The fluorescence resolution given in the captions is the theoretical bandpass at half-power of the fluorescence spectrometer calculated from the product of the slit width and the reciprocal linear dispersion. The measured bandpass corresponds closely. With a single exception, the highest energy structure in fluorescence (to the right) is also the position of excitation. That position is marked with an asterisk. The band intensity at that location is derived from fluorescence and scattered exciting light, and both are attenuated by reabsorption. Elsewhere the peak heights are a linear function of fluorescence intensity, and the spectra are fairly accurate representations of the relative band intensities.

Table I. Observed Vibrational Frequencies for the $^1A_{1g}$ and $^1B_{2u}$ States of C_6H_6 Vapor

Mode[a]	Symmetry species	Fundamentals,[b] cm^{-1}	
		$^1A_{1g}$	$^1B_{2u}$
1 (2)	a_{1g}	993.1[c]	923.0[d]
2 (1)	a_{1g}	3073	3130[e,f]
3 (3)	a_{2g}	1350	
4 (8)	b_{2g}	707	~365[f]
5 (7)	b_{2g}	990	749[f]
6 (18)	e_{2g}	608.0[g,h]	522.4[g]
7 (15)	e_{2g}	3056	3077.2[g,f]
8 (16)	e_{2g}	1599[i]	
9 (17)	e_{2g}	1178	~1148[f]
10 (11)	e_{1g}	846	585[e,f]
11 (4)	a_{2u}	674.0	514.8[g]
12 (6)	b_{1u}	1010	
13 (5)	b_{1u}	3057	
14 (9)	b_{2u}	1309	
15 (10)	b_{2u}	1146	
16 (20)	e_{2u}	398.6[g]	237.3[g]
17 (19)	e_{2u}	967	712[d,f]
18 (14)	e_{1u}	1037	
19 (13)	e_{1u}	1482	
20 (12)	e_{1u}	3064	

[a] Wilson's numbering: E. B. Wilson, Jr., *Phys. Rev.*, 45, 706 (1934). Herzberg's numbering is in parentheses: G. Herzberg, "Infrared and Raman Spectra", Van Nostrand, Princeton, N.J., 1945, p 118. [b] $^1A_{1g}$ fundamentals from S. Brodersen and A. Langseth, *Kgl. Dan. Vidensk. Selsk., Mat.-Fys. Skr.*, **1**, 1 (1956), except where noted. [c] Correction to ref 20 misprint. [d] G. H. Atkinson and C. S. Parmenter, unpublished results. [e] Reference 23. [f] Reference 18. [g] Reference 20. [h] Vibrational constants derived in ref 20 give $2\nu_6''$ $(l = 0) = 1219.4$ cm^{-1} and $2\nu_6''(l = 2) = 1219.7$ cm^{-1}. The vibrational angular momentum splitting in both the ground and excited electronic states is too small to be of significance in the fluorescence spectra of this report. [i] Unperturbed value after correction[29] for observed Fermi resonance with $(\nu_1'' + \nu_6'')$. The perturbed value is $\nu_8'' = 1590$ cm^{-1}. See reference in footnote *b* above.

(The fluorescence detection sensitivity drops by only about 15% as fluorescence is scanned to the limit of structure at large displacements from excitation.) The base or "zero fluorescence" signal is photomultiplier dark current which can generally be seen in the structureless region near excitation.

The markers under the fluorescence spectra identify members of progressions in ν_1. The assignment of each marker is given to the right with the changes in v_1'' usually omitted. Thus to each assignment must be added the component 1_n^m where m is v_1' in the emitting level (either 0, 1, or 2), and where n increases 0, 1, 2, . . . for successive markers counting always from zero at the right-hand (high energy) marker.

References to fluorescence band displacement describe the energy difference between the fluorescence band and the maximum of the absorption transition being pumped. Except where noted, fluorescence is at lower energy than excitation. Observed displacements are tabulated only for bands in zero-point fluorescence, which were recorded with best resolution. This spectrum required ~100 hr of scan time. Other spectra have been recorded more quickly at the expense of resolution and S/N. The locations of band maxima are thus less reproducible, often with an uncertainty of ± 10 cm^{-1}, and the maxima can be measured to this accuracy on the figures themselves.

Wavelength or wave number scales have generally been omitted from the figures, but the position of excitation is given in each caption and the displacement of any fluorescence band from that position can be derived quickly from the assignment markers. The latter show *calculated* displacements and do not attempt to "fit" band maxima. Thus the separation between markers in every progression is the

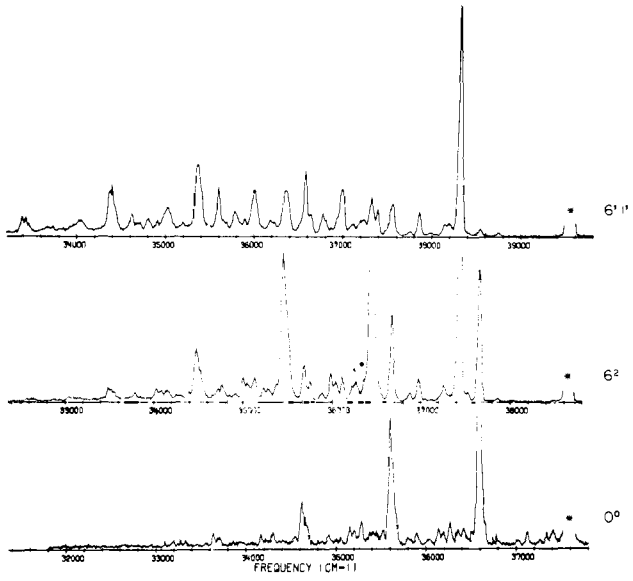

Figure 1. Fluorescence spectra from the levels $6^1 1^1$, 6^2, and 0^0 top to bottom. The spectra have been aligned with respect to the position of excitation which is marked with an asterisk. These spectra are linear in wave number. The control of band intensities by Franck-Condon factors can readily be seen by comparing bands in the spectra from 6^2 and $6^1 1^1$. The strong band closest to excitation in the 6^2 spectrum is conspicious by the relative absence of intensity at that displacement in the $6^1 1^1$ spectrum above it. These differences are a consequence of variation in the respective overlap integrals $\langle \phi_1''(1) | \phi_1'(0) \rangle$ and $\langle \phi_1''(1) | \phi_1'(1) \rangle$. We are indebted to Dr. Kenneth Tang for these spectra.

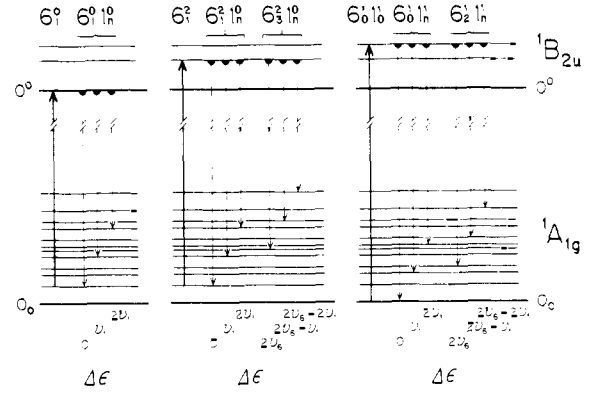

Figure 2. A schematic of the prominent fluorescence bands in the three spectra of Figure 1. Excitation and fluorescence for the levels 0^0, 6^2, and $6^1 1^1$ are shown left to right. The energy displacements $\Delta\epsilon$ of fluorescence bands from excitation are given below the band position in terms of the ground state vibrations ν_1'' (993 cm^{-1}) and ν_6'' (608 cm^{-1}). The vibrational levels in the ground state and excited state are scaled by energy. It is seen that the displacement of the prominent progression in 0^0 emission is matched in 6^2 and $6^1 1^1$ emission even though in the latter neither the initial level nor the terminating levels of fluorescence are in common with those of 0^0 fluorescence. A second intense progression beginning with a displacement of $2\nu_6''$ occurs in 6^2 and $6^1 1^1$ fluorescence, but it is precluded in 0^0 fluorescence by vibrational selection rules. In an analogous manner common displacements occur among the weaker structure in SVL spectra, but selection rules and other intensity restrictions cause some displacements seen in one SVL spectrum to be absent in another.

993 cm^{-1} fundamental of ν_1'' (anharmonicity being ignored). The displacement of the progression origin marker can be readily calculated using the vibrational frequencies in Table I.

The figures showing analyzed fluorescence spectra generally contain an insert showing the absorption spectrum at 0.5–2 cm^{-1} resolution in the region of excitation together with the intensity profile of the exciting light. The positions and band widths of excitation are drawn to scale, with the bandpass at half-power equivalent to the triangle base. The absorption spectra have increasing absorption downward with energy increasing to the right.

General Aspects of Fluorescence from Single Vibronic Levels

Fluorescence spectra from the levels 0^0, 6^2, and $6^1 1^1$ are compared in Figure 1. It is seen that each spectrum is unique and characteristic of the emitting level. The structure lies in different frequency regions and appears distinctive upon even casual inspection. Furthermore, the spectra are sparse in structure when compared to a higher pressure fluorescence spectrum[6] where vibrational equilibration occurs before emission, or to a 300°K absorption spectrum.[3]

In these respects, the spectra in Figure 1 are representative of most SVL spectra from benzene. Their simplicity testifies to success in producing fluorescence from molecules with vibrational population severely biased to a single level rather than a thermal array of levels. Their uniqueness reflects the ability to select that level by excitation of appropriate absorption bands.

Figure 1 also shows another aspect of SVL spectra. When the spectra are aligned with respect to the position of excitation, it is seen that the positions of many fluorescence bands are also aligned. The displacements from excitation of fluorescence bands measured in wave numbers fall within a limited set of values common to many spectra.

The origin of this effect is conveniently described by considering the photon energy balance in an SVL fluorescence experiment. Incident photons first pump molecules from a low vibrational level in the ground state (generally the zero-point level) to a particular vibronic level in the excited state. The excited molecules subsequently decay by emission from this level back to the ground state, but the fluorescence transitions usually terminate in vibrational levels higher than that initially pumped. Thus the absorption–fluorescence cycle effectively takes molecules from lower to higher ground state vibrational levels.

On an energy basis, this cycle "transfers" energy from the excitation photon to ground state vibrations. This photon energy loss appears as the energy difference between excitation and fluorescence, i.e., a displacement of fluorescence to lower energy from excitation. While such displacements are the rule in molecular fluorescence, only in SVL and in "resonance" fluorescence are those displacements a simple function of ground state vibrations.

Since the displacements in SVL spectra are ground state fundamentals, overtones, and combinations, they are independent of the excited state which happens to be intermediate to the absorption–fluorescence cycle. For this reason, displacements appearing in the fluorescence structure from many different levels form a common set. Furthermore, the size of that set is limited by vibrational degeneracies and by restrictions on vibronic activity so that the spectra are relatively sparse in structure.

A schematic description of prominent structure in three SVL spectra is shown in Figure 2 to illustrate the origin of common displacements.

Each SVL spectrum derives its uniqueness from intensity restrictions on individual transitions. These restrictions are governed by Franck–Condon factors and at least qualitatively by Herzberg–Teller controls on vibronic activity. Such restrictions are quite specific to the excited level from which fluorescence originates, and their effect on the appearance of spectra is, in some instances, spectacular. For example, compare 6^2 and $6^1 1^1$ emission in Figure 1. The fluorescence band at a displacement equal to ν_1'' in emis-

sion from the level $6^1 1^1$ is almost absent, whereas the corresponding band in 6^2 emission is intense. The latter derives from an upper level with $v_1' = 0$ for which the Franck-Condon factor $|\langle\phi_1''(1)|\phi_1'(0)\rangle|^2$ is appreciable. On the other hand, the band in $6^1 1^1$ emission is a $v_1' = 1 \rightarrow v_1'' = 1$ transition which recognizes Smith's prediction[24] of near cancellation in the $\langle\phi_1''(1)|\phi_1'(1)\rangle$ overlap integral.

Further discussions of these intensity factors in the benzene spectrum are given in the next sections. For these discussions and for subsequent analyses of spectra it is useful to note that every fluorescence transition of significant intensity is either a member of a progression in the symmetrical ring breathing mode ν_1, or it is the origin of the progression itself with $v_1'' = 0$. The relative intensities of members *within* a progression are set by Franck-Condon factors for ν_1. On the other hand, the intensity of the progression origin and hence of the entire progression relative to other progressions is principally a function of the Herzberg-Teller relationships for vibronically induced transitions.

Vibronic Activity in the $^1B_{2u}$–$^1A_{1g}$ Transition. The first successful analysis of the absorption spectrum[25,22] and all subsequent extensions of the analysis have documented the success of the Herzberg-Teller theory as at least a qualitative description of the vibronic acquisition of electric dipole intensity. Similarly consistent vibronic activity is also seen in the high-pressure vapor fluorescence[22] and in every SVL fluorescence spectrum so far published. Thus while quantitative tests of Herzberg-Teller predictions remain sparse, it is clear that the vibronic selection rules satisfactorily account for at least the bulk of the structure. A brief summary of this vibronic activity is now given as a basis for subsequent discussion of the SVL spectra in both parts I and II of this report.

The Herzberg-Teller description of vibronic activity may be displayed by expanding the electric dipole transition moment in normal nuclear coordinates Q_i about the ground state equilibrium geometry. For a vibronic state described by a Born-Oppenheimer product wave function $\Psi_e\phi_1 \ldots \phi_{20}$ (where $\phi_1 \ldots \phi_{20}$ are the vibrational wave functions associated with an electronic state whose wave function is Ψ_e), the transition moment is

$$R = \langle\Psi_e''\phi_1'' \ldots \phi_{20}''|\ \mu|\Psi_e'\phi_1' \ldots \phi_{20}'\rangle$$

which upon expansion about $Q_i = 0$ becomes

$$R = (M)_0\langle\phi_1'' \ldots \phi_{20}''|\phi_1' \ldots \phi_{20}'\rangle + \sum_i \left(\frac{\partial M}{\partial Q_i}\right)_0 \langle\phi_1'' \ldots \phi_{20}''|Q_i|\phi_1' \ldots \phi_{20}'\rangle + \tfrac{1}{2}\sum_i\sum_j \left(\frac{\partial^2 M}{\partial Q_i \partial Q_j}\right)_0 \langle\phi_1'' \ldots \phi_{20}''|Q_iQ_j| \times \phi_1' \ldots \phi_{20}'\rangle + \tfrac{1}{6}\sum_i\sum_j\sum_k \left(\frac{\partial^3 M}{\partial Q_i \partial Q_j \partial Q_k}\right)_0 \times \langle\phi_1'' \ldots \phi_{20}''|Q_iQ_jQ_k|\phi_1' \ldots \phi_{20}'\rangle + \text{higher order terms}$$

where $M = \langle\Psi_e''|\mu|\Psi_e'\rangle$.

The zero-order term $(M)_0 = \langle\Psi_e''(A_{1g})|\mu|\Psi_e'(^1B_{2u})\rangle$ vanishes by symmetry since $\Gamma(\mu)$ is $a_{2u}(\mu_z)$ or $e_{1u}(\mu_x,\mu_y)$. The remaining terms, however, can give rise to perpendicular (in-plane) transitions for vibrations fulfilling the following symmetry requirements

$$\text{first-order term, } \Gamma(Q_i) = e_{2g}$$

$$\text{second-order term, } \Gamma(Q_i) \times \Gamma(Q_j) \supset E_{2g}$$

$$\text{third-order term, } \Gamma(Q_i) \times \Gamma(Q_j) \times \Gamma(Q_k) \supset E_{2g}$$

Table II. Vibronic Activity for First- and Second-Order Herzberg–Teller Transitions in the $^1B_{2u}$–$^1A_{1g}$ System of Benzene

Order of H–T term	Transition	Allowed vibrational species	Observed examples
First	$X^n_{n\pm1}$	e_{2g}	6^1_0; 6^1_2
Second	$X^n_{n\pm2}$	e_{1g}; e_{1u}; e_{2g}; e_{2u}	16^2_0
Second	X^n_n (with $n > 0$)	e_{1g}; e_{1u}; e_{2g}; e_{2u}	10^1_1
Second	$X^n_{n\pm1}Y^m_{m\pm1}$	$e_{1g} \times b_{2g}$; $e_{1g} \times e_{1g}$ $e_{1u} \times b_{1u}$; $e_{1u} \times b_{2u}$ $e_{1u} \times e_{1u}$; $e_{2g} \times a_{1g}$ $e_{2g} \times a_{2g}$; $e_{2g} \times e_{2g}$ $e_{2u} \times a_{2u}$; $e_{2u} \times e_{2u}$	$11^1_0 16^1_0$; $11^1_0 16^0_1$

These terms describe the mixing of the $^1B_{2u}$ electronic state with the higher $^1E_{1u}$ state for which the transition $^1E_{1u} \leftrightarrow {}^1A_{1g}$ is symmetry allowed. The transitions so far identified in absorption and fluorescence correspond to these terms, and in fact the bulk of the assignments derive from only first- and second-order components.

The allowed first- and second-order vibronic activity is summarized in Table II which is adapted from CDM. The activity in Table II constitutes the Herzberg-Teller predictions (to first and second order) of specific vibrational changes capable of *inducing* transitions. In addition, each of these transitions can be accompanied by other vibrational activity which occurs as simple Franck-Condon activity. Thus any inducing transition may appear along with an even quantum change in a nontotally symmetric vibration and any quantum change in a symmetric mode. For example, the transition $6^1_0 11^2_0 1^1_0$ seen in absorption is a first-order transition induced by the e_{2g} mode ν_6 with changes in v_{11} and v_2 occurring as Franck-Condon activity.

Limited guidance is available from calculation concerning the relative intensities of the progression origins allowed within the constraints of symmetry. Attempts to calculate relative intensities are reported only for the first-order transitions 6^1_0, 7^1_0, 8^1_0, and 9^1_0, and it is perhaps surprising to note that of these, experimental intensity measurements are in the literature for only 6^1_0 and 7^1_0. Furthermore, these are only rough estimates from photographic plates of absorption.

On the other hand, the qualitative picture of relative intensities is comprehensive. From the previous analyses of absorption and fluorescence, order of magnitude intensities are available for many types of transitions, and they show severe restraints on vibronic activity in addition to the symmetry selection rules. It is first seen that only 12 of the 20 vibrations, representing only about half of the symmetry species, are "active" in transitions. Vibrations in the remaining species appear constrained to zero quantum changes. Of course not all of the structure in any benzene spectrum has been assigned so that transitions in some of these "inactive" modes may yet be found, albeit with low intensity. However, at the present moment, analyses including those in these reports have so far identified as "active" only the vibrations in Chart I. Vibrational activity varies substantially among the active modes.

Chart I

Symmetry	Vibration	Symmetry	Vibration
a_{1g}	ν_1, ν_2	e_{1g}	ν_{10}
b_{2g}	ν_4, ν_5	a_{2u}	ν_{11}
e_{2g}	ν_6, ν_7, ν_8, ν_9	e_{1u}	ν_{16}, ν_{17}

(1) The e_{2g} vibration ν_6 induces transitions whose intensities exceed by an order of magnitude those induced by other modes or by combinations of modes. On a relative basis, the first-order ν_6 transitions are the only strong transitions in

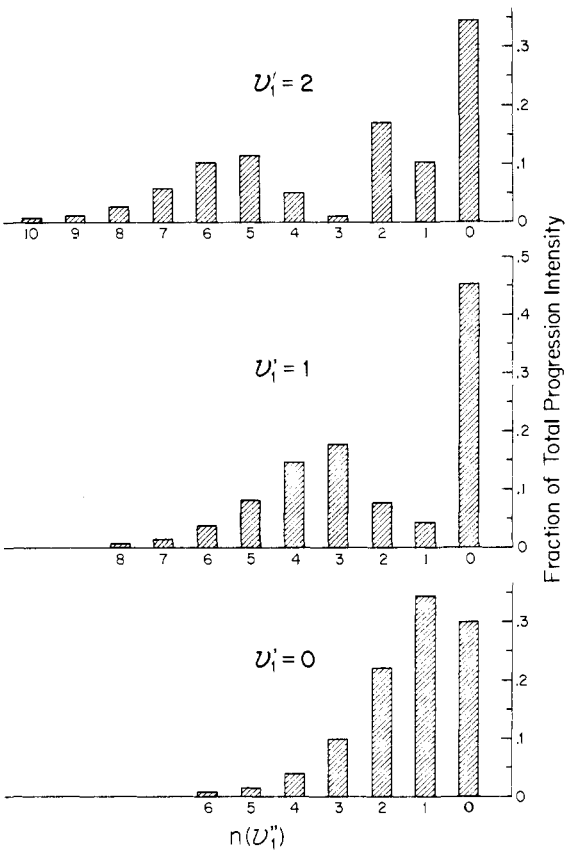

Figure 3. Calculated intensities within ν_1 progressions. The progressions are 1_n^0, 1_n^1, and 1_n^2 from bottom to top, respectively.

benzene spectra. The dominant progressions both in fluorescence and absorption are those with $\Delta v_6 = \pm 1$ and $\Delta v = 0$ in all other vibrations except ν_1 with which the progression is built. For example, this dominance is readily apparent in the 0^0 and 6^2 spectra of Figure 1. The single strong progression in 0^0 fluorescence and the two dominant progressions in 6^2 fluorescence are each $\Delta v_6 = \pm 1$ transitions. Only the $+1$ transition 6_1^0 can occur in the former spectrum whereas both $+1$ and -1 transitions (6_3^2 and 6_1^2) are expected from the level 6^2.

(2) The remaining structure (or alternatively, the weak structure) is based principally on four types of progression origins. (a) First-order transitions with $\Delta v = \pm 1$ in ν_7 or ν_9 and with $\Delta v = 0$ in all other nontotally symmetric modes. (b) First-order transitions with $\Delta v_6 = \pm 1$ combined with an even change in a nontotally symmetric mode. The transition $6_0^1 10_0^2$ seen in absorption can be considered an example of this type, with the segment 10_0^2 occurring as a Franck-Condon component to the change in v_6 which induces the transition. (For quantitative comparisons one would strictly need to consider some transitions of this type as gaining intensity both from the first-order component as described above and from a third-order term where together the activity in ν_6 and ν_{10} can contribute to the band intensity.) (c) Second-order transitions in which Δv_x and Δv_y each equal ± 1 with $\Delta v = 0$ in all other nontotally symmetric vibrations. The absorption band $10_0^1 4_1^0$ is of this class. The symmetry constraints on ν_x and ν_y are described in Table II. (d) Second-order transitions in which $\Delta v_x = \pm 2$ with $\Delta v = 0$ in all other nontotally symmetric modes. The 16_0^2 absorption band is of this type. Table II describes the symmetry constraints.

Franck-Condon Factors in Benzene Fluorescence. The a_{1g} vibration ν_1 is a ring breathing mode in which the principal motion is C-C modulation. The ring expansion upon $^1B_{2u} \leftarrow {}^1A_{1g}$ excitation causes this vibration to be active in

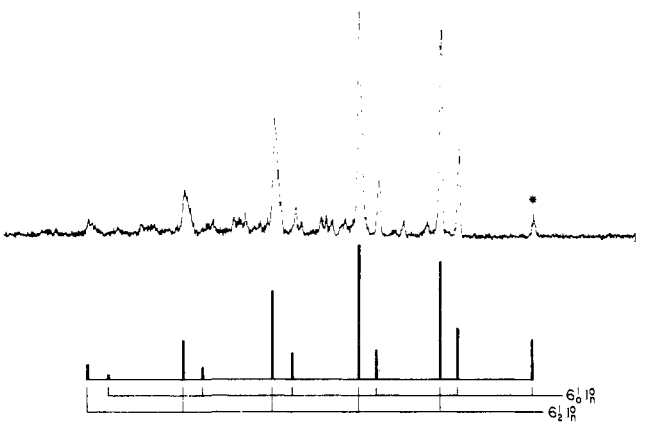

Figure 4. Fluorescence from the level 6^1 showing the ν_1 progressions $6_0^1 1_n^0$ and $6_2^1 1_n^0$. The calculated relative intensities within each progression are shown by the height of the vertical markers.

long progressions. The relative intensities of progression members are described approximately by the appropriate Franck-Condon overlap integrals, and these in turn are a function of the ν_1 frequencies in the two electronic states and the change in the C-C bond length upon excitation. Craig[26] used these relationships to calculate the C-C change from the relative intensities of absorption bands appearing in progressions with the components 1_0^n ($n = 0, 1, 2, \ldots$). Subsequent rotational analyses of absorption bands,[20] and other estimates summarized in CDM, give similar values (0.036-0.038 Å) for the C-C change.

Because of Boltzmann factors, only progressions with components 1_0^n and 1_1^n can be seen in absorption, and the latter was characterized only recently after a specific search among the more obscure absorption structure.[24] Even so, the members $\ldots 1_1^1$ and $\ldots 1_1^2$ of that progression remain too weak to identify.

Fluorescence gives a more extensive view of ν_1 progressions. Levels with $v_1' = 0$, 1, and 2 can be pumped selectively, and accordingly progressions with components 1_n^0, 1_n^1, and 1_n^2 occur in the resulting fluorescence.

To compare the intensity envelopes of these progressions with theory, we have reversed the procedure of Craig, and have calculated the progression intensity profiles from the parameters Δr(C-C) = 0.037 Å, $\nu_1' = 923$ cm^{-1}, and $\nu_1'' = 993$ cm^{-1}. The calculation has been made from Henderson's tables[27] of Franck-Condon factors. The calculated profiles are shown in Figure 3, where it is apparent immediately that qualitative differences in the three progressions should be present. The 1_n^0 progression is compact, falling to one-tenth the maximum value by the fifth member. It has its maximum in its second member (1_1^0) with no single member of dominant intensity. In contrast, the 1_n^1 progression is more extended and contains an unmistakable signature in its first two members. Almost half its intensity appears in the first while the second member is a comparatively vacant minimum. Finally, the 1_n^2 progression has two minima and is even further extended with significant intensity remaining in its ninth member.

Experimental examples of these progressions are given in the spectra of Figures 4, 5, and 6. The *calculated* progression intensities from Figure 3 are scaled over the progression markers to facilitate comparison with observed intensities. In every case the correspondence is good. The 1_1^0 maximum in the $v_1' = 0$ progression, the dominant and retiring natures of the first and second members respectively of the $v_1' = 1$ progression, and the extended envelope of the $v_1' = 2$ progressions each replicate the predictions of the calculations.

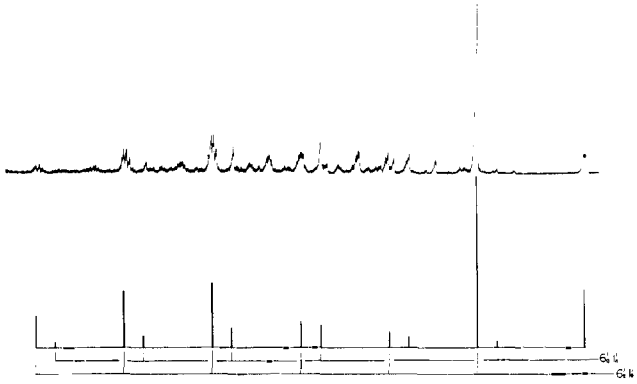

Figure 5. Fluorescence from the level $6^1 1^1$ showing the ν_1 progressions $6_0^1 1_n^1$ and $6_2^1 1_n^1$. The calculated relative intensities are shown by the height of the vertical markers. The spectrum is linear in wave number.

The intensities of two weak transitions deserve special attention. Smith[24] has shown how cancellation effects in Franck-Condon integrals operate to restrict the intensity of 1_1^1 progression members in benzene, and the spectrum from $6^1 1^1$ in Figure 5 demonstrates how effective that cancellation is. The $6_0^1 1_1^1$ transition, which lies in a region free of other structure, barely rises above the base line with an intensity ~2% that of the predominant $6_2^1 1_0^1$ transition. Likewise, $6_2^1 1_1^1$ (which is in fact a Fermi doublet) is scarcely discernible between two neighboring progression origins but estimates from higher resolution spectra[28,29] yield the correct intensity relative to $6_0^1 1_1^1$. Thus, while the approximate calculations indicate a deep minimum for these two progression members, they still overestimate their relative intensity by a factor of five. More exact calculations which take account of anharmonic contributions to progression intensities are in excellent agreement with the observed data.[28]

The distinctive appearances of these three progression types are valuable in SVL fluorescence analyses. Comparison of observed band intensities with the expected progression contours often allows a decision between assignments whose displacements are nearly coincident but which have different locations of their progression origins. In some cases, it has even been possible to evaluate quantitatively the contribution of various nearly coincident progressions by fitting the measured intensities to the predicted progression profile.

Perhaps an even more important use of the distinctive progression profiles is to identify the entwined fluorescence from two or more emitting levels differing in v_1'. Extensive use of this was made in analysis of the resonance fluorescence excited in benzene by absorption of light from the 2537 Å Hg line.[15] This technique also contributed[16] to the identification of the weak 17_0^2 absorption band in the region of the very strong absorption $6_0^1 1_0^1$ (see below).

Zero-Point Fluorescence

The zero-point level is reached by pumping the hot absorption band 6_1^0. The resulting fluorescence spectrum in Figure 7 has been recorded with sufficient S/N and narrow bandpass (4 cm^{-1}) so that the fluorescence resolution is about an order of magnitude greater than that in our previous report.[14] Positions of well defined band maxima can be located to ±1.5 cm^{-1}, and the rotational contours of many bands can be discerned clearly. The latter are comparable to the contours observed in absorption[20] since emission occurs from molecules with near-Boltzmann rotational distributions.

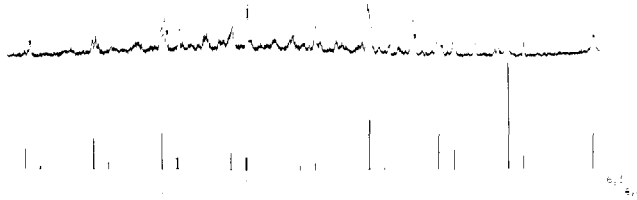

Figure 6. Fluorescence from the level $6^1 1^2$ showing the ν_1 progressions $6_0^1 1_n^2$ and $6_2^1 1_n^2$. The calculated relative intensities are shown by the height of the vertical markers. The spectrum is linear in wave number.

Band maxima are identified in Figure 7 by their displacement from the $B_0^0(6_1^0)$ band maximum at 37,482 cm^{-1}. Frequencies and assignments of those maxima are listed in Table III.

The Origin 6_1^0. The first member (6_1^0) of the dominant progression, $6_1^0 1_n^0$, is obscured by scattered exciting light. The strongest band in the spectrum, $6_1^0 1_1^0$, would be expected to lie at −993 cm^{-1}. However, two bands appear astride this position. They arise due to the well known Fermi resonance involving ν_8'' and ($\nu_6'' + \nu_1''$). Subsequent members of the progression $6_1^0 1_n^0$ also appear as doublets and, indeed, any transition terminating in a level which includes a $6_1 1_1$ component (e.g., $6_1 10_2 1_1$) appears as a doublet.

Two other progression origins predicted to lie near $6_1^0 1_1^0$ were thought earlier to contribute toward the intensity in this region.[14] The origin 16_4^0 is calculated to lie at −992 cm^{-1} (when corrections for anharmonicity are included). In Figure 7, only an indistinct shoulder on the low-energy side of the Fermi component at −988 cm^{-1} marks the expected position for 16_4^0. However, spectra taken with increased resolution confirm the presence of a weak band at −993 cm^{-1}. We assign this to be the origin of the progression $16_4^0 1_n^0$. The progression member $16_4^0 1_1^0$ has been observed with somewhat greater clarity at −1986 cm^{-1}.

The origin $11_1^0 17_1^0$, predicted to lie at −1033 cm^{-1}, is not observed. Presumably it is hidden in the extended rotational envelope of $6_1^0 1_1^0$. In absorption, the analogous transition $11_0^1 17_0^1$ can be observed, although it is among the weaker second-order transitions.

No satisfactory assignment has been found for the band at −974 cm^{-1} which lies toward higher energy from the $6_1^0 1_1^0$ Fermi component at −988 cm^{-1}. The band at −1949 cm^{-1} also has not been assigned. We presume that they arise as a result of excitation of weak absorption bands near B_0^0 but further identification has not been pursued.

The Origin $4_1^0 10_1^0$. The combination band $4_1^0 10_1^0$ typifies a second-order transition of type $X_{m\pm1}^m Y_{n\pm1}^n$ where, in this case, $\Gamma_x \times \Gamma_y = b_{2g} \times E_{1g} \supset E_{2g}$. The progression $4_1^0 10_1^0 1_n^0$ was not identified in the earlier analysis,[14] and this transition finds precedent only in the analogous cross sequence $4_1^0 10_0^1$ proposed by CDM as a possible assignment for one of the bands in the absorption group H_0^0. Our observations substantiate this assignment by confirming that the b_{2g} mode ν_4, in combination with ν_{10}, is active in inducing the $^1B_{2u} \leftrightarrow {}^1A_{1g}$ transition.

In fluorescence, the observed displacement for $4_1^0 10_1^0$ (−946 cm^{-1}) is in close agreement with the calculated displacement of −945 cm^{-1}. No splitting is observed for progression members for which $v_1'' \geq 1$, thus confirming that $v_6'' = 0$ for this transition. (If the transition was of the type $6_1^0 X_m^0$, then $6_1^0 1_1^0 X_m^0$ and higher progression members would display the characteristic splitting due to the ($\nu_6'' + \nu_1''$) . . . ν_8'' Fermi resonance.) We note, however, that the band $4_1^0 10_1^0 1_1^0$ appears more intense than expected from Franck-Condon considerations. The added intensity is due

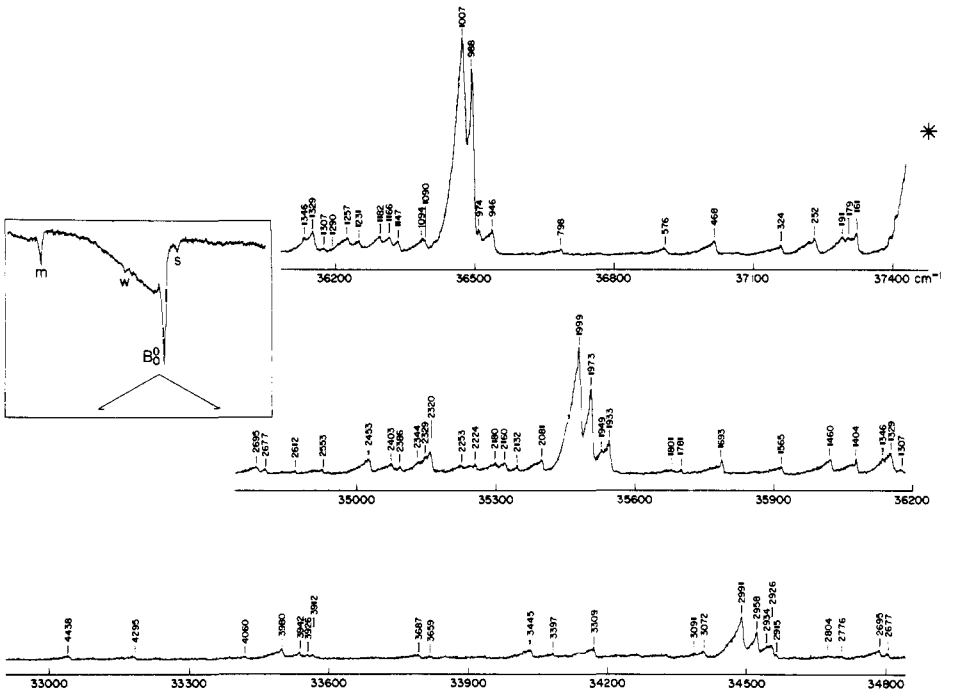

Figure 7. Fluorescence from the $^1B_{2u}$ zero-point level excited by pumping the $6_1^0(B_0^0)$ absorption band. Bands are labeled according to their displacement from the 6_1^0 band maximum at 37,482 cm^{-1}. Band positions and assignments are given in Table III. The spectrum is linear in wave number. Excitation is centered at 37,475 cm^{-1} with 85 cm^{-1} bandpass. Fluorescence bandpass is 4 cm^{-1}. Due to degradation in lamp intensity during the scanning period (100 hr), fluorescence at longer wavelengths appears weaker than expected relative to fluorescence occurring nearer to excitation. Emission from $6^1 16^1$ is also present due to simultaneous pumping of the absorption $6_0^1 16_1^1 1_1^0$ whose maxima (w) lie ~25 cm^{-1} lower in energy than the B_0^0 band maximum. Absorption bands: m, 37,392.5, 37,392.7 cm^{-1} (D_0^0:6_2^1); w, 37,452.5, 37,457.3 cm^{-1} ($6_0^1 16_1^1 1_1^0$); s, 37,490.6 cm^{-1}.

to a new progression whose origin is coincident with $4_1^0 10_1^0 1_1^0$, namely $6_1^0 17_2^0$. Further discussion follows below.

The analogous transition $4_0^1 10_0^1$ in absorption has now been located via SVL excitation. The details are discussed in the following paper.

ν_5 is also of species b_{2g} and would therefore be expected to appear in combination with ν_{10} just as does ν_4. The calculated position for the origin $5_1^0 10_1^0$ (−1228 cm^{-1}) coincides with the transition $6_1^1 16_1^1 8_1^0$. (The latter arises due to excitation of the weak hot band $6_0^1 16_1^1 1_1^0$ which lies in the rotational tail of 6_1^0). No significant intensity additional to that expected for $6_1^1 16_1^1 8_1^0$ appears at this displacement. We conclude that $5_1^0 10_1^0$ is considerably weaker than $4_1^0 10_1^0$.

The Origins 16_2^0, 17_2^0, $16_1^0 17_1^0$. Benzene has two e_{2u} fundamentals, ν_{16} and ν_{17}, which can each induce intensity in the $^1B_{2u}$–$^1A_{1g}$ transition according to the selection rule $\Delta v = \pm 2$. This is a second-order Herzberg-Teller transition of type $X_{m\pm 2}^m$ where the symmetry component e_{2g} is contained in $(e_{2u})^2$. It follows that the combination band $16_1^0 17_1^0$ is also symmetry allowed since $e_{2u} \times e_{2u} \supset E_{2g}$.

The transition 16_2^0 in absorption[20,21,30] lies at 37,289.9 cm^{-1}. Our value of 37,291 cm^{-1} for the fluorescence transition is in close accord. Figure 7 shows two transitions, at −161 cm^{-1} and −179 cm^{-1}, with rotational tails overlapped by 16_2^0 (−191 cm^{-1}). The former can be assigned securely as $6_1^0 16_1^1$. Its presence in 0^0 fluorescence is due to upward vibrational relaxation to the level 16^1 which lies at 0 + 237 cm^{-1}. Spectra taken at lower pressures show diminished intensity in this progression. A satisfactory assignment has not been found for the progression headed by the band at −179 cm^{-1}.

The prominent progression beginning with the band at −1329 cm^{-1} was originally[3] thought to be $6_1^0 11_2^0 1_n^0$ but later[14] interpreted as $17_2^0 1_n^0$. The latter assignment is now confirmed. The measured displacement yields $\nu_{17}'' = 968$ cm^{-1}, which compares with the infrared measurement of 967 cm^{-1}. The nearby progression $6_1^0 16_2^2 1_n^0$ arises as a result of upward vibrational relaxation to the level 16^2. The intensity relative to $6_1^0 16_1^1 1_n^0$ is consistent with this proposal.

An exceedingly weak band appears at the calculated position (−759 cm^{-1}) for $16_1^0 17_1^0$. Satisfactory evidence exists for this transition in absorption (see part II) but we are led to conclude that in fluorescence the transition is considerably weaker than either 16_2^0 or 17_2^0.

The Origin $11_1^0 16_1^0$. The sole a_{2u} fundamental, ν_{11}, can appear as a second-order transition in combination with an e_{2u} mode, ν_{16} or ν_{17}. The cross sequence, $11_1^0 16_0^1$, is well represented in absorption, and $11_1^0 16_1^0$ is seen clearly in 0^0 fluorescence. Our measured position, 37,014 cm^{-1}, compares with the value 37,016 cm^{-1} obtained from the analysis of hot bands in absorption.[20,21,30]

The transition $11_1^0 17_1^0$ calculated at −1033 cm^{-1} does not emerge obviously from the rotational tail of $6_1^0 1_1^0$, although a weak shoulder is apparent at this position in Figure 7. In absorption, the intensity of $11_0^1 17_0^1$ is reported greater than $11_0^1 16_0^1$ by a factor of 3.[21,30] There is therefore an apparent discrepancy between the relative strengths of the $(\nu_{11} + \nu_{16})$ and $(\nu_{11} + \nu_{17})$ combination bands in emission and in absorption.

The Origin 10_2^0. The second-order transition 10_0^2 is seen clearly in absorption, and the fluorescence band at −1090 cm^{-1} is assigned as 10_2^0. The calculated displacement is −1084 cm^{-1}. The 6-cm^{-1} difference between the observed and calculated value is too large to be attributed solely to experimental error. Repeated scans of the −1090-cm^{-1} band suggest that there are two or more overlapping transitions in this region. However, the next progression member, $10_2^0 1_1^0$, does not seem as broad in the region near its maximum and its observed displacement (−2081 cm^{-1}) is nearer the calculated value of −2077 cm^{-1}. The intensities of the progression members $10_2^0 1_n^0$ are consistent with the expected Franck-Condon envelope but we cannot reconcile the observed discrepancy in band positions.

The Origin $6_1^0 10_2^0$. A well-defined band at −1693 cm^{-1}

Table III. Bands Observed in Fluorescence from the Zero-Point Level of Benzene Vapor

Band max, cm^{-1}(vac)	Displacement,[a] cm^{-1}	Assignment	Comments	Band max, cm^{-1}(vac)	Displacement,[a] cm^{-1}	Assignment	Comments
37,321	161	$6_1^0 16_1^1$; $6_1^0 11_1^1$	From vibrational relaxation	35,401	2081	$10_2^0 1_1^0$	
				35,350	2132	$8_1^0 16_1^1 1_1^0$; $8_1^0 11_1^1 1_1^0$	
37,303	179			35,322	2160	$6_1^0 16_1^1 1_2^0$; $6_1^0 11_1^1 1_2^0$	
37,291	191	16_2^0	Gives $2\nu_{16}'' = 797$ cm^{-1}	35,302	2180	$16_2^0 1_2^0$	
37,230	252	$6_2^1 16_1^1$	from excitation of $6_0^1 16_1^1 1_1^0$	35,258	2224	$6_2^1 8_1^0 16_1^1 1_1^0$	
				35,229	2253	$6_2^1 16_1^1 1_2^0$	
37,158	324	$6_1^0 16_2^2$; $6_1^0 11_1^1 16_1^1$	From vibrational relaxation	35,162	2320	$17_2^0 1_1^0$	
				35,153	2329	$8_1^0 11_2^0$	
37,014	468	$11_1^0 16_1^0$		35,138	2344	$6_1^0 11_2^0 1_1^0$	
36,906	576	9_1^0	Gives $\nu_9'' = 1182$ cm^{-1}	35,096	2386		$\nu_1'' = 1$ progression member, related to origin at -1404 cm^{-1}
36,684	798	$6_1^0 16_2^0$					
36,536	946	$4_1^0 10_1^0$		35,079	2403		
36,508	974			35,029	2453	$11_1^0 16_1^0 1_2^0$; 7_1^0	
36,494	988[b]	8_1^0		34,929	2553	$9_1^0 1_2^0$	
36,489	993	16_4^0	Confirmed at higher resolution	34,870	2612		$\nu_1'' = 1$, related to -1620 cm^{-1}
36,475	1007	$6_1^0 1_1^0$		34,805	2677	$8_1^0 10_2^0$	
36,392	1090	10_2^0	Gives $2\nu_{10}'' = 1696$ cm^{-1}	34,787	2695	$6_1^0 10_2^0 1_1^0$	
36,388	1094			34,706	2776	$8_1^0 16_2^0 1_1^0$	
36,335	1147	$8_1^0 16_1^1$; $8_1^0 11_1^1$		34,678	2804	$6_1^0 16_2^0 1_2^0$	
36,316	1166	$6_1^0 16_1^1 1_1^0$; $6_1^0 11_1^1 1_1^0$		34,567	2915		
36,296	1186	$16_2^0 1_1^0$		34,556	2926	$4_1^0 10_1^0 1_2^0$; $6_1^0 17_2^0 1_1^0$	
36,251	1231	$6_1^1 8_1^0 16_1^1$		34,548	2934		
36,225	1257	$6_1^1 16_1^1 1_1^0$		34,524	2958	$8_1^0 1_2^0$	
36,192	1290	$8_1^0 16_2^2$		34,491	2991	$6_1^0 1_3^0$	
36,175	1307	$6_1^0 16_2^2 1_1^0$		34,410	3072	$10_2^0 1_2^0$	
36,153	1329	17_2^0	Gives $2\nu_{17}'' = 1935$ cm^{-1}	34,391	3091		
36,136	1346	$6_1^0 11_2^0$	Gives $2\nu_{11}'' = 1346$ cm^{-1}	34,173	3309	$17_2^0 1_2^0$	
36,078	1404			34,085	3397		$\nu_1'' = 2$, related to -1404 cm^{-1}
36,022	1460	$11_1^0 16_1^0 1_1^0$					
35,917	1565	$9_1^0 1_1^0$		34,037	3445	$11_1^0 16_1^0 1_3^0$; $7_1^0 1_1^0$	
35,789	1693	$6_1^0 10_2^0$		33,823	3659	$8_1^0 10_2^0 1_1^0$	
35,701	1781	$8_1^0 16_2^0$		33,795	3687	$6_1^0 10_2^0 1_2^0$	
35,681	1801	$6_1^0 16_2^0 1_1^0$		33,570	3912		
35,549	1933	$4_1^0 10_1^0 1_1^0$; $6_1^0 17_2^0$		33,556	3926		
35,533	1949			33,540	3942	$8_1^0 1_3^0$	
35,509	1973	$8_1^0 1_1^0$		33,502	3980	$6_1^0 1_4^0$	
35,496	1986	$16_4^0 1_1^0$	Confirmed at higher resolution	33,422	4060		
				33,187	4295	$17_1^0 1_3^0$	
35,483	1999	$6_1^0 1_2^0$		33,044	4438	$7_1^0 1_2^0$	Minor contribution from $11_1^0 16_1^0 1_4^0$

[a] Observed position of $6_1^0(B_0^0)$ absorption band maximum (37,481.6 cm^{-1}) minus measured position of fluorescence band maximum. [b] Fermi doublets are bracketed.

matches the calculated position (-1692 cm^{-1}) of the transition $6_1^0 10_2^0$. The next two progression members appear as Fermi doublets approximately astride the "unperturbed" $6_1^0 10_2^0 1_n^0$ positions, confirming that the terminating level is a combination involving ν_6'' and that the band at -1693 cm^{-1} is the progression origin ($\nu_1'' = 0$). No evidence can be found in this region for the transition $6_1^0 4_1^0 5_1^0$ calculated at -1697 cm^{-1}.

The Origin $6_1^0 11_2^0$. The progression $6_1^0 11_2^0 1_n^0$ was not confirmed previously in fluorescence from the zero-point level. ν_{11} is of species a_{2u} and therefore contributes only Franck-Condon intensity in this transition. In Figure 7 it can be seen that $6_1^0 11_2^0$ is overlapped by the rotational tail of 17_2^0 which lies toward higher energy. However, the observed displacement (-1346 cm^{-1}) agrees satisfactorily with the calculated value (-1348 cm^{-1}). In absorption, the progression K_n^0 is assigned securely as $6_0^1 11_0^2 1_0^n$.

The Origins $6_1^0 16_2^0$ and $6_1^0 17_2^0$. These transitions, together with $6_1^0 10_2^0$, comprise a set for which intensity can in principle be derived both from the first-order term, where X_2^0 is a Franck-Condon component, and a third order term arising due to $e_{2g} \times (\Gamma_x)^2 \supset E_{2g}$ for $\Gamma_x = e_{1g}$ or e_{2u}.

The progression origin $6_1^0 16_2^0$ is found to coincide exactly with the calculated position (anharmonic corrections included) of -798 cm^{-1}. Higher progression members are split by the $(\nu_6'' + \nu_1'') \ldots \nu_8''$ interaction, as would be expected for this transition.

$6_1^0 17_2^0$ (calculated at -1934 cm^{-1}) is nearly coincident with $4_1^0 10_1^0 1_1^0$ (calculated displacement -1938 cm^{-1}) and has been mentioned in our prior discussion. The second progression member $6_1^0 17_2^0 1_1^0$ is expected to appear as a Fermi doublet and indeed one does observe a band (-2915 cm^{-1}) at the appropriate displacement for the higher energy Fermi component, $8_1^0 17_2^0$ (calculated -2917 cm^{-1}). The intensity of the progression $6_1^0 17_2^0 1_n^0$ appears less than one-third the intensity of $4_1^0 10_1^0 1_n^0$.

The Origins 7_1^0 and 9_1^0. The progression origin 7_1^0 (calculated -2448 cm^{-1}) would be nearly coincident with $11_1^0 16_1^0 1_2^0$ (calculated -2451 cm^{-1}). However, additional intensity in excess of that expected from Franck-Condon con-

siderations for $11_1^0 16_1^0 1_2^0$ is seen at -2435 cm^{-1}, and this is consistent with the appearance of the new progression origin, 7_1^0. Subsequent progression members, $7_1^0 1_1^0$ and $7_1^0 1_2^0$, are seen also.

The progression origin 9_1^0 is observed at -576 cm^{-1} but without a well-defined band maximum. It is difficult to position the band origin, but an estimate yields $\nu_9'' = 1182$ cm^{-1}. The next progression member (-1565 cm^{-1}) has a more clearly defined maximum giving $\nu_9'' = 1178$ cm^{-1} The infrared value (vapor) is $\nu_9'' = 1178$ cm^{-1}. $9_1^0 1_2^0$ is observed at -2553 cm^{-1} but is less distinct.

Analogous progressions for both ν_7 and ν_9 have been assigned in absorption[20,21,30] and the absorption origins 7_0^1 and 9_0^1 have been confirmed by SVL fluorescence (see part II).

Fluorescence from Levels with Excitation in ν_6 and ν_1

Members of the progressions $6_0^1 1_0^n(A_n^0)$, $6_1^0 1_0^n(B_n^0)$ and $6_1^2 1_n^0(C_n^0)$ are among the most intense bands in the $^1B_{2u} \leftarrow {}^1A_{1g}$ absorption spectrum so that there is good opportunity to see fluorescence from levels with excitation in ν_1 and ν_6. Unfortunately, not all of the excited states reached by these bands can be pumped uniquely. While the A_n^0 and C_n^0 bands are fairly free of congestion, B_n^0 progression members with $n \geq 1$ are overlapped by the bands of the much stronger $A_n^1(6_0^1 16_1^1 1_0^n)$ progression. Thus a clear picture of emission from levels with excitation in ν_1 alone cannot be obtained easily by pumping the B_n^0 bands. The SVL spectra displayed in this section are from levels with excitation either in ν_6 alone or in ν_6 in combination with ν_1.

6^1 Emission after $6_0^1(A_0^0)$ Absorption. This spectrum, shown in Figure 8, is characteristically dominated by $\Delta v_6 = \pm 1$ transitions. They appear here as the progressions $6_0^1 1_n^0$ and $6_2^1 1_n^0$ whose origins are separated by $2\nu_6'' = 1219$ cm^{-1}. Their relative intensities are typical of that seen throughout benzene SVL spectra. The integrated intensity in the $6_2^1 1_n^0$ progression measured from higher resolution spectra[28] is found to be approximately 2.5 times that in the progression $6_0^1 1_n^0$. This is to be compared with the ratio expected from the Herzberg–Teller transition moment integrals describing those progressions

$$\frac{\text{intensity in } 6_2^1 1_n^0}{\text{intensity in } 6_0^1 1_n^0} \approx \frac{|\langle 6^1 | Q_6 | 6_2 \rangle|^2}{|\langle 6^1 | Q_6 | 6_0 \rangle|^2}$$

where the functions 6^1, 6_2, and 6_0 are vibrational eigenfunctions for the degenerate coordinate Q_6. The ratio reduces to exactly three if a single set of harmonic oscillator eigenfunctions are used for both electronic states.

Even a simple comparison of peak heights shows that this expectation is approximately realized. The ratio is so consistently between two and three in spectra where assignments are secure that it is used as an additional criterion when discussing a difficult assignment. If say, a $6_0^1 X_2^2$ progression is proposed, its consort $6_2^1 X_2^2$ must also be present with at least double the intensity.

Assignment of the weak fluorescence structure has been accomplished in part by comparison with our more detailed analysis of 0^0 fluorescence. Knowledge of Franck–Condon factors and of the presence (or absence) of related progressions contributes to the security of assignments. These criteria are of assistance where there is a choice among close assignments and where the measurements of band position are not sufficiently precise to allow assignment on the basis of frequency alone. Assignments so chosen establish a consistent pattern of vibronic activity among the weak structure in the various SVL fluorescence spectra and in the absorption spectrum.

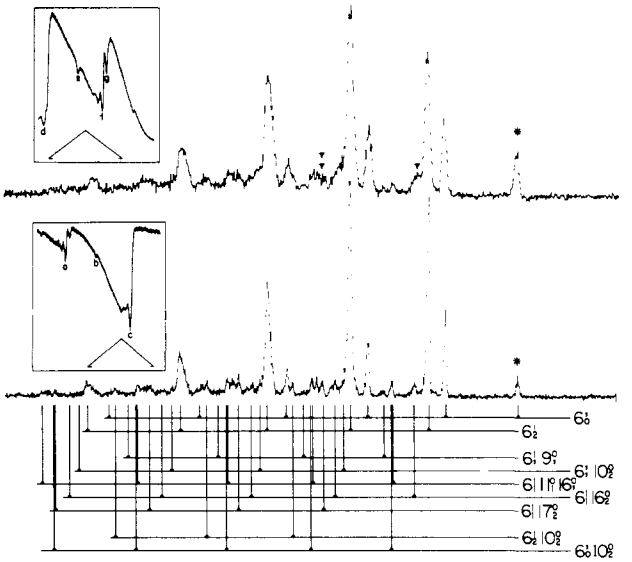

Figure 8. Bottom: fluorescence from 6^1 excited by pumping $6_0^1(A_0^0)$ in absorption. To every assignment must be added 1_n^0. Fluorescence bandpass is 20 cm^{-1}. Excitation is centered at 38,600 cm^{-1} with 45 cm^{-1} bandpass. Absorption bands: a, 38,522.5 cm^{-1} (C_0^0:6_1^2); b, 38,562.4 cm^{-1} (I_0^0:16_0^2); c, 38,611.3 cm^{-1} (A_0^0:6_0^1). Top: fluorescence from 6^2 excited by pumping $6_1^2(C_0^0)$ in absorption. The spectrum has been aligned above the 6^1 spectrum according to the position of excitation, and the linear wavelength dispersion is the same for both. Fluorescence bandpass is 75 cm^{-1}. Excitation is centered at 38,500 cm^{-1} with 40 cm^{-1} bandpass. Absorption bands: d, 38,452 cm^{-1} (A_0^0:$6_0^1 16_1^1$); e, 38,491 cm^{-1}; f, 38,522.5 cm^{-1} (C_0^0:$6_1^2 I_1^0$); g, 38,529.3 cm^{-1} ($C_0^0 6_1^2 I_1^2$).

The minor structure in the 6^1 spectrum is induced by transitions of two types. The progression origins are summarized in Chart II.

Chart II

$6_1^1 7_1^0$	
$6_1^1 9_1^0$	$6_0^1 10_2^0$, $6_2^1 10_2^0$
$6_1^1 10_2^0$	$6_0^1 11_2^0$, $6_2^1 11_2^0$
$6_1^1 11_1^0 16_1^0$	$6_0^1 16_2^0$, $6_2^1 16_2^0$
$6_1^1 16_2^0$	$6_0^1 17_2^0$, $6_2^1 17_2^0$
$6_1^1 17_2^0$	
$6_1^1 4_1^0 10_1^0$	

Progressions with $\Delta v_6 = 0$ can be distinguished because they stand alone without the pairwise relationships found in $\Delta v_6 = \pm 1$ progressions. Many progression origins with $\Delta v_6 = 0$ are found among the weak bands in SVL fluorescence as well as absorption. For example, the progression origins 7_1^0, 9_1^0, 10_2^0, 16_2^0, 17_2^0, $11_1^0 16_1^0$, and $4_1^0 10_1^0$ are all present in zero-point fluorescence, and their counterparts are assigned in absorption (see part II). In 6^1 fluorescence, these types of progression origins would appear in combination with 6_1^1, and as an ensemble, they comprise the bulk of fluorescence intensity not contained in the two main progressions 6_2^1 and 6_0^1. Analogs of all the $\Delta v_6 = 0$ progression origins seen in zero-point fluorescence have been confirmed in 6^1 fluorescence from spectra taken at higher resolution.[29] In Figure 8, only those progression origins seen unambigiously at the present resolution have been included. Splittings due to Fermi resonance are not resolved.

The progression origins $6_{0,2}^1 10_2^0$ are analogous to progressions of the type $6_0^1 X_0^2$ seen in absorption where X is ν_{10}, ν_{11}, ν_{16}, and ν_{17}. However only the transitions in ν_{10} appear prominent at the resolution used for Figure 8. As in absorption, the intensties of the ν_{10} fluorescence transitions are

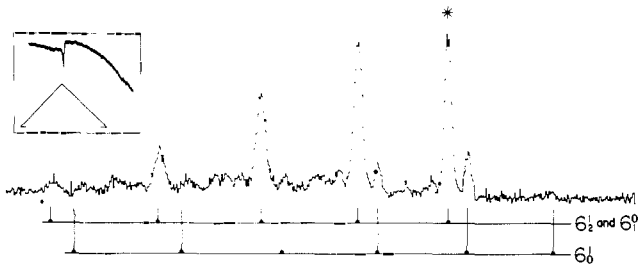

Figure 9. Fluorescence from 6^1 excited by pumping the $6_2^1(D_0^0)$ absorption band which is overlapped by the $6_1^0(B_0^0)$ absorption band. To each emission assignment must be added 1_n^0. Note that the excitation position in this unique case is not at the high energy edge of the fluorescence structure. The fluorescence bandpass is 75 cm^{-1}. Excitation is centered at 37,390 cm^{-1} with a 50 cm^{-1} bandpass. The sharp maximum in the absorption spectrum is the D_0^0 band at 37,392.6 cm^{-1}. The absorption at higher energy to the right is the rotational tail of the B_0^0 band. Some emission from the zero-point level is present as the progression $6_1^0 1_n^0$.

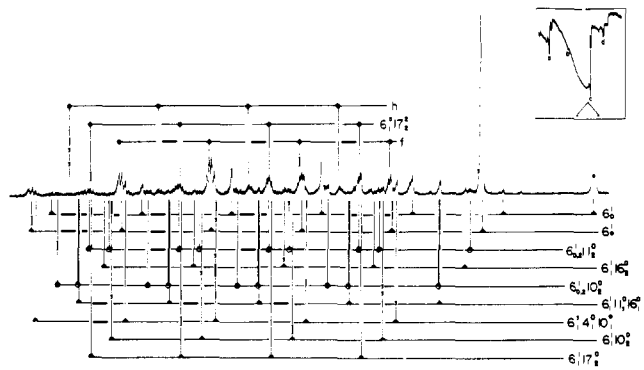

Figure 10. Fluorescence from $6^1 1^1$ excited by pumping $6_0^1 1_0^1(A_1^0)$ in absorption. To every assignment of emission from the level $6^1 1^1$ must be added 1_n^1. Progressions h and f originate from other excited states. The progression $6_1^0 17_0^2 1_n^0$ originates from simultaneous pumping of the absorption band 17_0^2 lying 10 cm^{-1} toward lower energy from absorption maximum "c". Fluorescence bandpass is 7 cm^{-1} and the spectrum is linear in wave number. Excitation is centered at 39,529 cm^{-1} with a 45 cm^{-1} bandpass. Absorption bands: a, 39,444.6 cm^{-1} (C_1^0:$6_1^2 1_0^1$); b, 39,487 cm^{-1} (I_1^0:$16_0^2 1_0^1$); c, 39,534.6 cm^{-1} (A_1^0:$6_0^1 1_0^1$); d, 39,560.6 cm^{-1}.

weak compared with the progressions built on $\Delta v_6 = \pm 1$ changes alone. The relative intensities of the $6_2^1 10_2^0$ and $6_0^1 10_2^0$ progressions in Figure 8 are not in good agreement with the approximate ratio 3:1 expected from the Herzberg-Teller integrals. Higher resolution spectra[29] show that the progression $6_1^1 11_1^0 16_1^0$ is responsible. It is coincident at our resolution with the progression $6_0^1 10_2^0$.

6^1 Emission after $6_2^1(D_0^0)$ Absorption. The D_0^0 absorption band is weak due to its Boltzmann factor of about 0.004 at room temperature, and it lies on the rotational tail of the much stronger $6_1^0(B_0^0)$ absorption band. Accordingly the spectrum in Figure 9 contains contributions from the zero-point level as well as from the level 6^1 and it is shown at low fluorescence resolution due to low intensity. In spite of these shortcomings, the spectrum is included here because it is the best opportunity to see emission from the same upper state (6^1) reached by two different absorption bands (6_0^1 and 6_2^1). It also offers a novel opportunity to generate resonance emission at higher energy than the exciting line.

The 6^1 spectra in Figures 8 and 9 show the expected equivalence. Aside from the reduced resolution in Figure 9, the two differ only in the relative intensities of their $6_2^1 1_n^0$ and $6_0^1 1_n^0$ progressions. The former is considerably enhanced in Figure 9 because the $6_2^1 1_n^0$ progression merges with the $6_1^0 1_n^0$ progression of the "contaminating" zero-point level fluorescence. By comparison with Figure 8, it is estimated that about 20% of the "$6_2^1 1_n^0$ intensity" is due to zero-point emission.

The 6^1 emission generated by pumping 6_2^1 absorption should show fluorescence to higher energy than excitation via the $6_0^1 1_n^0$ fluorescence progression. The members $6_0^1 1_0^0$ and $6_0^1 1_1^0$ will be displaced $+ 2v_6'' = +1219$ cm^{-1} and $+ 2v_6'' - v_1'' = +226$ cm^{-1} from the excitation line, respectively. The $6_0^1 1_0^0$ band in fluorescence is attenuated by reabsorption, but the second fluorescence band at +226 cm^{-1} is clearly visible.

Fluorescence from 6^2 Excited by Pumping $6_1^2(C_0^0)$. A priori expectations suggest that both the displacements and the relative intensities of progressions in SVL fluorescence from the levels 6^2 and 6^1 will match closely. For every progression in 6^1 fluorescence an analogous progression should occur in fluorescence from 6^2. A few examples are given in Chart III.

These expectations are substantiated by the comparison of 6^2 and 6^1 fluorescence in Figure 8. Aside from the lower resolution of the 6^2 spectrum, upon alignment the two appear nearly identical.

The most pronounced deviation is a progression in 6^2 fluorescence beginning at -1350 cm^{-1}. The intensity at that position (marked in Figure 8 with a single pip) is enhanced in 6^2 fluorescence.

Chart III

Progression origin from 6^1	Progression origin from 6^2	Displacement from excitation 6_0^1 or 6_1^2
6_0^1	6_1^2	Zero
6_2^1	6_3^2	$-2v_6'' = -1219$ cm^{-1}
$6_0^1 10_2^0$	$6_1^2 10_2^0$	$-2v_{10}'' = -1692$
$6_1^1 16_2^0$	$6_2^2 16_2^0$	$-(v_6'' + 2v_{16}'') = -1406$

The enhancement is due to emission from a second level, 11^2, pumped when trying to reach the single level 6^2 by the absorption bands 6_1^2. The 6_1^2 bands are overlapped by the absorption $6_1^0 11_0^2$ whose maximum at 38,517.4 cm^{-1} is just 5 cm^{-1} away from one of the 6_1^2 maxima.[15,31,32] One expects that the most intense emission from 11^2 is that in which $\Delta v_6 = \pm 1$ and $\Delta v_x = 0$ for all other asymmetric vibrations. Thus the single progression $6_1^0 11_2^2 1_n^0$ should dominate 11^2 fluorescence, and in the presence of fluorescence from other excited levels, this would be the only clearly recognizable progression. That progression, whose origin is at $2v_{11}'' = -1348$ cm^{-1}, matches the position of the anomalously intense progression in the 6^2 spectrum.

Support for assigning structure from 11^2 also derives from trying to attribute it to the excited state 6^2. From that state, the progression $6_1^2 11_2^0$ could most reasonably account for the -1348 cm^{-1} displacement of the progression origin, but it would demand that a second progression $6_3^2 11_2^0$ whose origin is at -2564 cm^{-1} be also present with at least twice the intensity. This position is marked with double pips in Figure 8, and structure with such intensity is absent.

An interesting aside concerns the relative intensities at the positions of excitation in Figure 8. Reabsorption by the transition 6_0^1 reduces the intensity in the 6^1 spectrum whereas the unfavorable Boltzmann factor for the absorption 6_1^2 precludes appreciable reabsorption in the 6^2 spectrum.

$6^1 1^1$ Emission after $6_0^1 1_0^1(A_1^0)$ Absorption. The addition of the symmetric ring breathing mode v_1 to an emitting level dramatically changes the spectrum. Compare, for example, the $6^1 1^1$ spectrum in Figure 10 with the 6^1 spectrum in Figure 8. At first inspection, they hardly seem related.

The transformation is due almost entirely to Franck-Condon factors for v_1. As the emitting level changes from 6^1 to $6^1 1^1$, the v_1 progressions in fluorescence change from type 1_n^0 to 1_n^1, and the relative intensities of the members

within each are completely different. As described previously, the 1_n^0 progression climbs to maximum intensity in its 1_1^0 member and then drops smoothly with larger n. In contrast, the intensity of the first member of the progression 1_n^1 exceeds by more than a factor of 2 the intensity of any other member, and the intensity of its second member (1_1^1) is vanishingly small. Thus where the 1_n^0 progression has maximum intensity the 1_n^1 progression has almost zero intensity. For this reason an intense band at -993 cm^{-1} appears in 6^1 fluorescence (the band nearest to excitation) whereas it is almost absent in $6^1 1^1$ fluorescence.

Aside from Franck-Condon factors, the activity and relative intensity of progressions in $6^1 1^1$ fluorescence should approximately match those in 6^1 fluorescence and this seems to be the case. Most of the intensity in $6^1 1^1$ fluorescence occurs in the simple $\Delta v_6 = \pm 1$ progressions $6_2^1 1_n^1$ just as with 6^1 fluorescence. Again, one sees that the weak structure is derived from transitions of the type $6_{0,2}^1 X_2^0 1_n^1$ and of the type $6_1^1 X_2^0 1_n^1$ with the same modes active in the spectra from both levels. However, there are some differences between the two spectra which require comment.

Enhanced intensity appears in $6^1 1^1$ fluorescence at a displacement of -1350 cm^{-1} marked $6_0^1 1_2^0 1_0^1$. Other progression origins such as $6_0^1 16_1^0 17_1^0 1_0^1$ or possibly $6_0^1 3_0^0 1_0^1$ may also contribute intensity. The $\Delta v_6 = +1$ components of all these transitions lie near the rather strong $6_1^0 17_2^2 1_n^0$ progression discussed below. Presumably the concentration of intensity in progression origins of 1_n^1 progressions makes these weak transitions visible in $6^1 1^1$ emission whereas they escape detection in 6^1 fluorescence.

The absence of progression markers for $6_1^1 9_1^0 1_n^1$ in the $6^1 1^1$ spectrum does not indicate any fundamental change from either zero-point or 6^1 fluorescence. The progression origin $6_1^1 9_1^0$ can be seen clearly as a weak band between the bands $6_1^1 11_1^0 16_1^0 1_0^1$ and $6_0^1 1_2^1$. But the higher members of $6_1^1 9_1^0 1_n^1$ are obscured by a stronger progression "h" which is discussed below.

A prominent progression, $6_1^0 17_2^2 1_n^0$ occurs in $6^1 1^1$ fluorescence but has no counterpart in the 6^1 spectrum. It originates from the level 17^2 pumped via the 17_0^2 absorption band whose maximum lies ~ 10 cm^{-1} to the red of the $6_0^1 1_0^1$ absorption maximum. The 17_0^2 maximum is not listed in the compilation of absorption bands by Radle and Beck,[21] but at high resolution the $17_0^2 1_0^n$ progression can be seen in A_n^0 absorption bands beginning with the A_1^0 band.[30,31] The basis of the assignment is given by Atkinson.[30,31]

The fluorescence structure excited by this absorption is consistent with Atkinson's assignment. First, the Franck-Condon envelope of the fluorescence progression has maximum intensity in its second member so that the progression is clearly from an upper state with $v_1' = 0$. Second, the progression $6_1^0 17_2^2 1_n^0$ is expected to exceed the intensity of other progressions from 17^2 by an order of magnitude. It would be the only identifiable 17^2 structure in the presence of $6^1 1^1$ fluorescence. Some additional intensity appears at -2542 cm^{-1}, near $6_1^0 17_2^2$ (-2552 cm^{-1} from A_1^0), due to the first member of the progression $6_1^1 17_2^0 1_0^1$.

Two progressions which seem not to originate from the level $6^1 1^1$ remain in Figure 10. One whose origin is near 2775 cm^{-1} is labeled "h" in the assignments. Its Franck-Condon envelope identifies it as emission from an upper state with $v_1' = 0$ or else it is the unlikely coincidence of a $6^1 1^1$ progression beginning at -2775 cm^{-1} and another overlapping $6^1 1^1$ progression beginning at $-(2775 + 993)$ cm^{-1}. It cannot be satisfactorily assigned on this basis nor as 17^2 emission, and hence it appears to come from a *third* origin excited in absorption. No hint of the absorption band leading to this origin has come from examination of high resolution absorption spectra.

The other unassigned progression, labeled "f", has its origin at -2224 cm^{-1}. Its Franck-Condon envelope is difficult to discern due to higher progression members being overlapped by other transitions (including $6_2^1 1_n^1$). However, no counterpart to this progression is seen in either 0^0 or 6^1 emission. It is presumably emission from a state other than $6^1 1^1$.

Finally, the spectrum in Figure 10 is sufficiently well resolved to reveal the $(v_6'' + v_1'') \ldots v_8''$ Fermi resonances in transitions which terminate at levels composed of $(v_6'' + nv_1'')$ ($n > 0$). These splittings were not resolved in the 6^1 emission shown in Figure 8, but nevertheless, bands which are doublets do appear broadened in that spectrum.

$6^1 1^2$ Emission after $6_0^1 1_0^2 (A_2^0)$ Absorption. The addition of a second quantum of v_1 to 6^1 in the excited state causes a further change in the fluorescence spectrum. The fluorescence from $6^1 1^2$ shown in Figure 11 does not have the "open" appearance of 6^1 and $6^1 1^1$ fluorescence.

The analysis shows that this change is again due to the continued variation in Franck-Condon factors for the v_1 progression. Two minima (at $n = 2$ and 4) appear in 1_n^2 progressions and the first member, $n = 0$, is not as dominant as in the case of 1_n^1 progressions. Furthermore the intensity is distributed over a larger number of progression members. In 1_n^0 progressions, fluorescence is essentially limited to the first five members.[34] The distribution increases to about six members in 1_n^1 progressions and about eight members in 1_n^2 progressions. As a result the $6^1 1^2$ spectrum extends over a spectral range of about 9000 cm^{-1} compared to 5500 cm^{-1} and 6500 cm^{-1} for 6^1 and $6^1 1^1$ fluorescence, respectively.

The progressions $6_{0,2}^1 1_n^2$ are prominent in $6^1 1^2$ fluorescence, but the assignment of the weaker structure is more difficult because of congestion which derives from the long Franck-Condon envelopes. Nonetheless, the spectrum appears to be satisfactorily assigned with progressions analogous to those seen in 6^1 and $6^1 1^1$ fluorescence. There are two unassigned progressions in this spectrum. One of these, the progression h, was also present in $6^1 1^1$ fluorescence where it displayed the intensity contour of a $v_1' = 1$ progression. The second unassigned progression, labeled m, has a Franck-Condon envelope consistent with that of an emitting state with $v_1'' = 0$. This progression has no counterpart in 6^1 or $6^1 1^1$ emission.

The fluorescence from the level $17^2 1^1$ pumped along with the main absorption is prominent in the spectrum of Figure 11. Franck-Condon factors operate to boost the visibility of $17^2 1^1$ fluorescence in two ways. They first optimize pumping of $17^2 1^1$ in the presence of $6^1 1^2$ excitation. The excitation of $17^2 1^1$ is via absorption $17_0^2 1_0^1$ occurring at its progression maximum while the competing absorption $6_0^1 1_0^2$ is off the maximum of its $6_0^1 1_0^n$ progression. In excitation of $6^1 1^1$ emission for Figure 10 the absorption $6_0^1 1_0^1$ was at the maximum of its progression envelope while 17_0^2 was not. Second, the Franck-Condon envelope of $17^2 1^1$ fluorescence emphasizes that emission by placing dominant intensity in its first progression member. At the same time, the broad intensity envelope of the $v_1' = 2$ progressions makes $6^1 1^2$ fluorescence appear less intense in comparison with a more compact spectrum from another emitting level.

Fluorescence from Levels with Excitation in v_{16}

The e_{2u} mode v_{16} is the only vibration in benzene with a ground state frequency less than 600 cm^{-1}. Accordingly, it is the only mode active in forming sequence absorption bands of appreciable intensity at room temperature. Fortunately, the ground and upper state frequencies of v_{16} are sufficiently different so that sequence and parent bands can be pumped without mutual interference. For example, the sequence absorption $6_0^1 16_1^1$ lying 161 cm^{-1} below its parent

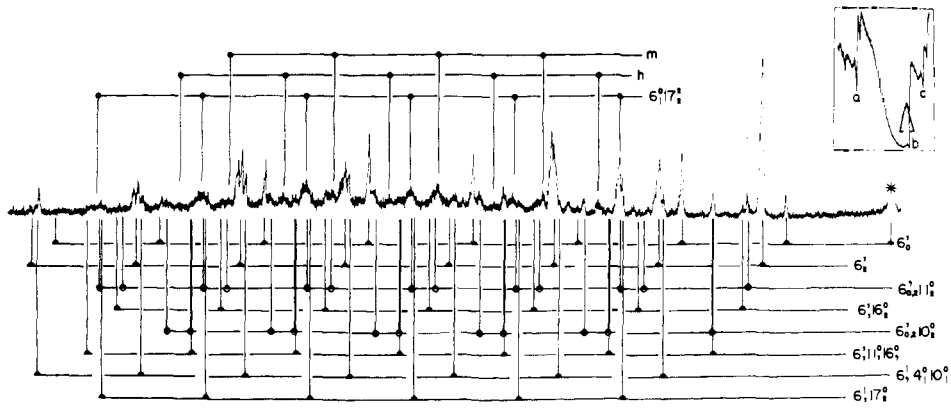

Figure 11. Fluorescence from $6^1 1^2$ excited by pumping the $6^1_0 1^2_0(A^0_2)$ absorption band. To every assignment of emission from the level $6^1 1^2$ must be added the component 1^2_n. Emission from three other levels is also present. The fluorescence progression $6^0_1 17^2_2 1^1_n$ is excited by pumping the $17^2_0 1^1_0$ absorption band 10 cm^{-1} to the red of absorption position "b". The progressions h and m each originate from other unidentified levels. Fluorescence bandpass is 13 cm^{-1} and the spectrum is linear in wave number. Excitation is centered at 40,455 cm^{-1} with a 20 cm^{-1} bandpass. Absorption bands: a, 40,366 cm^{-1} (C^0_2:$6^2_1 1^2_0$); b, 40,456.7 cm^{-1} (A^0_2:$6^1_0 1^2_0$); c, 40,480.7 cm^{-1}.

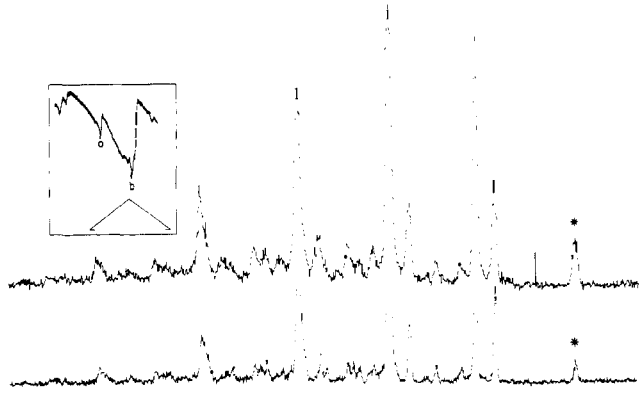

Figure 12. Fluorescence from $6^1 16^1$ excited by pumping the $6^1_0 16^1_1(A^1_0)$ absorption band (top) aligned over fluorescence from the 6^1 level (bottom) excited by pumping the $6^1_0(A^0_0)$ absorption band. For $6^1 16^1$ fluorescence, the fluorescence bandpass is 45 cm^{-1} and excitation is centered at 38,445 cm^{-1} with a 50 cm^{-1} bandpass. Absorption bands: a, 38,406.3 cm^{-1} (B^0_1:$6^0_1 1^1_0$); b, 38,452 cm^{-1} (A^1_0:$6^1_0 16^1_1$).

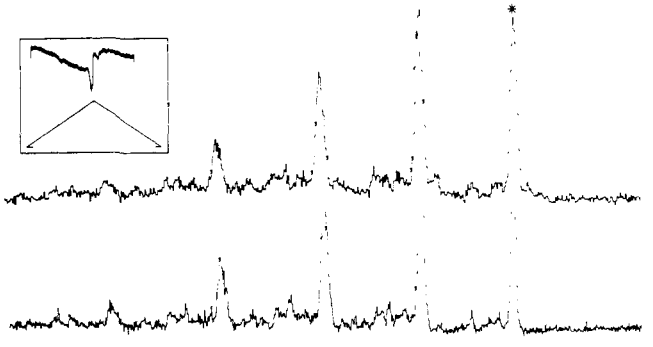

Figure 13. Fluorescence from 16^1 excited by pumping the $6^0_1 16^1_1(B^1_0)$ absorption band (top) aligned over fluorescence from the zero-point level (bottom) excited by pumping the $6^0_1(B^0_0)$ absorption band. For 16^1 fluorescence, the fluorescence bandpass is 75 cm^{-1}, and excitation is centered at 37,325 cm^{-1} with a 50 cm^{-1} bandpass. The sharp maximum in the absorption spectrum is that of the B^1_0 band at 37,321 cm^{-1}.

6^1_0 can be excited selectively to reach the level $6^1 16^1$. By analogous absorptions, a number of fluorescence spectra from an upper state X^nY^m can be compared with that from the state $X^nY^m 16^1$.

The SVL fluorescence spectrum generated by exciting a sequence band replicates in every case the spectrum obtained by pumping the parent band. The mode ν_{16} is Franck-Condon biased to $\Delta v_{16} = 0$, and every fluorescence from a "parent" state X^nY^m is simply mirrored by an analogous transition with the additional component 16^1_1 from its "sequence" state $X^nY^m 16^1$. Both the displacements and the relative intensities of fluorescence bands in "parent" spectra are replicated in "sequence" fluorescence. Two examples are offered.

$6^1 16^1$ Emission after $6^1_0 16^1_1(A^1_0)$ Absorption. Figure 12 compares fluorescence from the levels 6^1 and $6^1 16^1$ reached by pumping the 6^1_0 and $6^1_0 16^1_1$ absorption bands, respectively. Aside from greater noise and a slightly expanded intensity scale in the spectrum from $6^1 16^1$, the two spectra appear essentially identical when aligned according to their excitation positions. The $6^1 16^1$ spectrum would be uniformly displaced by 161 cm^{-1} to lower energy from 6^1 emission if presented at true wavelengths. The assignments describing the 6^1 spectrum in Figure 8 need only the added component 16^1_1 to describe correctly the $6^1 16^1$ spectrum.

16^1 Emission after $6^0_1 16^1_1(B^1_0)$ Absorption. Fluorescence from the level 16^1 and the zero-point level is compared in Figure 13. These spectra were obtained by pumping the sequence absorption $6^0_1 16^1_1$ and its parent band 6^0_1. Again the replication of structure is apparent, and the spectrum from 16^1 can be assigned by simply adding the component 16^1_1 to the zero-point assignments in Figure 7. It should be noted that the low intensity structure just to the right of the strong $6^0_1 16^1_1 1^0_n$ progression in 16^1 fluorescence has no counterpart in zero-point structure. At the slightly higher pressures used to obtain 16^1 fluorescence with a reasonable signal-to-noise ratio, collisions have taken about 5% of the 16^1 molecules to the zero-point level from which that emission derives. It is the origin of the zero-point progression $6^0_1 1^0_n$.

Summary

SVL fluorescence spectra offer a comprehensive view of the vibronically induced $^1B_{2u}$–$^1A_{1g}$ transition in benzene vapor. Useful generalities as well as new details have emerged from their analysis.

Vibronic Acquisition of Intensity. SVL fluorescence endorses the success of Herzberg-Teller theory in accounting for the bulk of the $^1B_{2u}$–$^1A_{1g}$ radiative transition probability. A single first-order Herzberg-Teller selection rule describes the dominant structure in every SVL spectrum we have obtained. The same rule governs the principal transitions in absorption. Higher order Herzberg-Teller selection rules provide an equally consistent account of the minor fluorescence structure. Finally, qualitative agreement is found between observed and Herzberg-Teller predicted fluorescence band intensities.

Vibronic Selection Rules. The dominant fluorescence structure from every emitting level appears to be predicted simply. It will be that for which the e_{2g} mode ν_6 changes quantum number by ± 1 while $\Delta v = 0$ for all other modes except ν_1. Changes in ν_1 establish long progressions on the ν_6 transition. We have observed no exceptions to this pattern.

The remaining fluorescence transitions are generally at least an order of magnitude weaker. They derive intensity from first-order Herzberg-Teller transitions involving e_{2g} modes other than ν_6, or more commonly they represent a limited selection of second-order transitions. These are summarized in the section Vibronic Activity in the $^1B_{2u}$–$^1A_{1g}$ Transition.

Franck–Condon Factors. The fluorescence spectra offer an extended view of polyatomic Franck–Condon factors. Numerous spectra display the relative intensities in ν_1 progressions of the types 1_n^0 and 1_n^1, and one spectrum shows the progressions 1_n^2. These three types are qualitatively different, and each matches the general expectations of approximate Franck–Condon calculations. The $\langle \phi_1''(1) | \phi_1'(1) \rangle$ overlap integral "cancellation" described by Smith is clearly seen. The great differences between 1_n^0, 1_n^1, and 1_n^2 progression envelopes is a principal contributor to the unique appearance of individual SVL fluorescence spectra.

Acknowledgment. We are indebted to Drs. George H. Atkinson and Kenneth Tang for numerous helpful discussions. We are also grateful for the National Science Foundation support of this work. The authors have benefited from fellowship support from the John Simon Guggenheim Foundation (C.S.P.), the National Aeronautics and Space Administration (M.W.S.), and the Lubrizol Corporation (M.W.S.) during part of this work.

References and Notes

(1) Contribution 2322 from the Chemical Laboratories of Indiana University. This work was supported by grants from the National Science Foundation.
(2) This work was supported by grants from the National Science Foundation.
(3) C. S. Parmenter and M. W. Schuyler, *J. Chim. Phys. Phys.-Chim. Biol., Suppl.*, 92 (1970).
(4) W. Gelbart, K. G. Spears, K. F. Freed, J. Jortner, and S. A. Rice, *Chem. Phys. Lett.*, **6**, 345 (1970).
(5) B. K. Selinger and W. R. Ware, *J. Chem. Phys.*, **53**, 3160 (1970); **52**, 5482 (1970).
(6) C. S. Parmenter and M. W. Schuyler, *Chem. Phys. Lett.*, **6**, 339 (1970).
(7) W. R. Ware, B. K. Selinger, C. S. Parmenter, and M. W. Schuyler, *Chem. Phys. Lett.*, **6**, 342 (1970).
(8) K. G. Spears and S. A. Rice, *J. Chem. Phys.*, **55**, 5561 (1971).
(9) W. Siebrand, *J. Chem. Phys.*, **54**, 363 (1971).
(10) D. F. Heller, K. F. Freed, and W. M. Gelbart, *J. Chem. Phys.*, **56**, 2309 (1972).
(11) C. S. Parmenter and M. D. Schuh, *Chem. Phys. Lett.*, **13**, 120 (1972).
(12) G. Herzberg and E. Teller, *Z. Phys. Chem., Abt. B*, **21**, 410 (1933).
(13) J. M. Blondeau and M. Stockburger, *Ber. Bunsenges. Phys. Chem.*, **75**, 450 (1971).
(14) C. S. Parmenter and M. W. Schuyler, *J. Chem. Phys.*, **52**, 5366 (1970).
(15) G. H. Atkinson, C. S. Parmenter, and M. W. Schuyler, *J. Phys. Chem.*, **75**, 1572 (1971).
(16) C. S. Parmenter, *Adv. Chem. Phys.*, **22**, 365 (1972).
(17) C. S. Parmenter and A. H. White, *J. Chem. Phys.*, **50**, 1631 (1969). The S_1 lifetimes are known to be less than 100 nsec[5,8] and while the collisional cross sections for vibrational relaxation in benzene–benzene collisions are large enough to initiate some relaxation at 0.15 Torr, only a careful and specific study can reveal its occurrence. With one exception, relaxation is not sufficient to bring appreciable emission intensity from levels not initially pumped.
(18) A. E. W. Knight, C. S. Parmenter, and M. W. Schuyler, *J. Am. Chem. Soc.*, following paper.
(19) G. H. Atkinson, C. S. Parmenter, and M. W. Schuyler. "Creation and Detection of the Excited State", Vol. 2, W. R. Ware, Ed., (Marcel Dekker).
(20) J. H. Callomon, T. M. Dunn, and I. M. Mills, *Philos. Trans. R. Soc. London, Ser. A*, **259**, 499 (1966).
(21) W. F. Radle and C. A. Beck, *J. Chem. Phys.*, **8**, 507 (1940).
(22) H. Sponer, G. Nordheim, A. L. Sklar, and E. Teller, *J. Chem. Phys.*, **7**, 207 (1939).
(23) F. M. Garforth and C. K. Ingold, *J. Chem. Soc.*, 417 (1948).
(24) W. L. Smith, *Proc. Phys. Soc., London, Sect. B*, **1**, 89 (1968).
(25) A. L. Sklar, *J. Chem. Phys.*, **5**, 669 (1937).
(26) D. P. Craig, *J. Chem. Soc.*, 2146 (1950).
(27) J. R. Henderson, *J. Chem. Phys.*, **41**, 580 (1964).
(28) K. Tang, unpublished results.
(29) A. E. W. Knight and C. S. Parmenter, unpublished results.
(30) G. H. Atkinson, Ph.D. Thesis, Indiana University, 1971.
(31) G. H. Atkinson and C. S. Parmenter, *J. Phys. Chem.*, **75**, 1564 (1971).
(32) The maxima g and f in Figure 8 are absorption bands $6_1^2 J_1^2$ and $6_1^2 J_1^0$ reaching the different angular momentum components of the level 6^2. The $6_1^0 11_0^2$ band is the maximum just to the left of band f.
(33) For example, see Figure 2 of ref 31.
(34) Fluorescence in higher members can be observed but well over 90% of a progression's intensity is contained in the first five members.

An Extended View of the Benzene 260-nm Transition via Single Vibronic Level Fluorescence. II. Single Vibronic Level Fluorescence as a Probe in the Assignment of the Absorption Spectrum[1,2]

A. E. W. Knight, C. S. Parmenter,* and M. W. Schuyler

Contribution from the Department of Chemistry, Indiana University, Bloomington, Indiana 47401. *Received September 9, 1974.*

Abstract: Twelve regions of the benzene 260-nm transition have been probed with narrow-band excitation to produce fluorescence spectra from single vibronic levels or small groups of levels of the $^1B_{2u}$ state. The fluorescence analyses identify many of the emitting levels and confirm or establish 28 $^1B_{2u} \leftarrow {}^1A_{1g}$ absorption assignments. Four new excited state fundamentals are located: $\nu_4' = 365$ cm^{-1}, $\nu_5' = 749$ cm^{-1}, ν_9' 1148 cm^{-1}, and $\nu_{17}' = 712$ cm^{-1}. A set of 12 vibrations encompassing six of the the ten symmetry species initiates most of the structure in the $^1B_{2u}$–$^1A_{1g}$ transition. Each vibration in these six species is "active".

Fluorescence spectra from a representative set of single vibronic levels (SVL) in the $^1B_{2u}$ state of benzene vapor have been analyzed in the preceding report.[3] Each spectrum was obtained by pumping an absorption band with a well established assignment so that the fluorescence analyses were based on secure knowledge of the emitting levels. Every spectrum followed a consistent pattern of vibronic activity which matched that seen in absorption. In this paper,